Radiation patterns of tsunami on static fault models

Radiation Patterns of Tsunami on Static Fault Models

Kuniaki ABE

Niigata Junior College, The Nippon Dental University

Hamaura-cho 1-8, Niigata 951, Japan

Abstract

Radiation patterns of tsunami at sea were shown using numerical simulations. The sources are a thrust fault and a strike-slip fault under the sea. Time histories of sea levels at points distant from the source of various azimuth directions were computed and analyzed into amplitude spectra. Azimuth dependencies of the maximum sea level and the most predominant frequencies were illustrated. As the result of the maximum level a symmetrical pattern for the thrust and a quadrant one for the strike-slip fault were obtained. The symmetrical pattern has no node but the quadrant one has two nodal lines which are perpendicular to each other. In the thrust model the strongest radiation is observed at directions normal to the fault strike.However, in the strike-slip model the strongest radiation is observed in intermediate directions between strike and the normal.As for the radiation patterns of the most predominant frequencies the highest ones in the thrust model and the lowest ones in the strike–slip model are obtained at the normal directions But in the latter case the result is not so systematic. Decrease of the maximum sea level due to propagation distance also depends on the azimuth.In the normal direction the decrease was very small and the small decrease explains the maximum radiation as the result. The radiation patterns suggest that a superposing condition has an important role in the tsunami arrival of high level.

Introduction

Directivity of tsunami has attracted much attention. In Japan it was noticed by Matsuzawa (1937) as an azimuthal variation of initial phase. After that it was studied by Miyoshi (1955), Momoi (1962) and Hatori (1963). Observed tsunami is affected by the propagation in addition to the source. In the discussion it is important to separate the effects into two. At the present stage the source is approximated by a fault model. A numerical experiment based on the fault model was carried out by Aida (1978) and the reliability was discussed. Analytical expression of the spectral amplitude of tsunami based on a fault model was given by Yamashita and Sato (1974).

It is shown by Abe (1993) that observed amplitude spectra are synthesized by source spectrum and shelf response. This idea led us to an inversion of fault model from the observed spectra (Abe and Okada, 1995 a, 1995 b and Abe, 1996). As for the inversion a comparison of waveform is also a useful method in numerical simulations.

Dip-slip fault has been known as the source of tsunami because of the large vertical displacement. A recent strike-slip fault, generated Kobe earthquake, 1995, accompanied a small tsunami (Abe and Okada, 1996). This fact gives us a motivation to classify the radiation patterns of tsunami into two according to the fault type. In this article we will study the radiation pattern in waveform and the spectra using numerical simulations at a constant-depth sea.

Numerical simulation and the parameters

Tsunami is approximated by linear long water wave without sea bottom resistance. The generation is attributed to the vertical displacement of sea bottom. The displacement field is equal to one derived by formula of Mansinha and Smylie (1971). It is assumed to be completed at rise time t_0. Thus the model is non-propagational in space and has a dependence of ramp function in time. The same numerical scheme as one used by Abe and Okada (1995 a) is used.

The model is applied to a contant-depth sea without land. Boundary condition at four margins is a usual transmission condition. The sea levels on the sea are computed step by step and the time histories are obtained. The time histories are analyzed into the amplitude spectra.

Definitions of parameters and the coordinate system are shown in Fig.1. The sea depth h_0 and rise time t_0 are assumed to be 2 km and 10 s, respectively. Since the rise time is very shory for tsunami to propagate and an assumption of instantaneous generation nolds as a good approximation.

As for the fault models two typical faults are considered. One is a thrust type with a low dip angle and pure dip-slip, and another is a strike-slip type with a high dip angle and pure strike-slip. The former is frequently seen in the north-east Japan and the latter is seeen at the sea region of Izu peninsula in Japan. The parameters are shown in Table 1. The upper margins of the assumed faults are assumed to be very shallow($d_0 = 1$ km) because of an appropriate condition of tsunami generation.
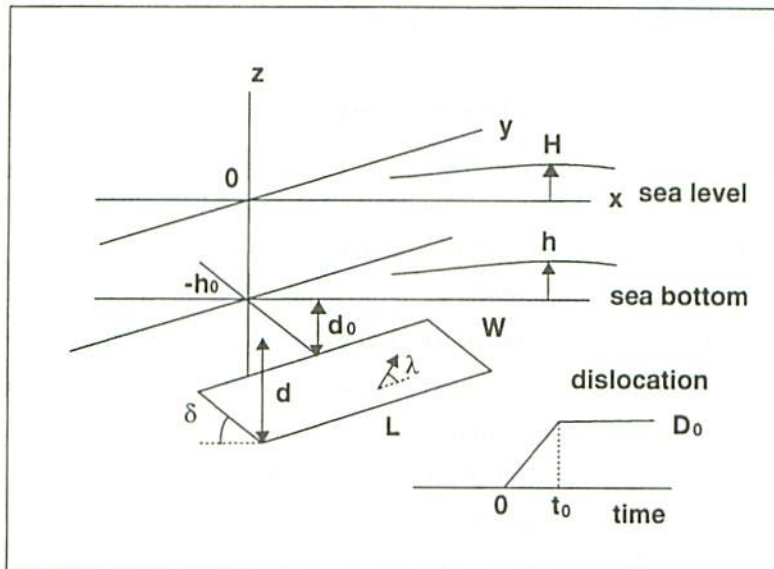

Fig.1   Coordinate system and parameters used in this work.

Parameter list

model	L(km)	W(km)	d_o(km)	D_o(m)	δ(°)	λ(°)
Thrust fault	50	25	1	1	30	90
Strike-slip fault	50	25	1	1	85	0

Table 1

A grid space, consisting of 400($Imax$)×380($Jmax$) grids, with the interval(Δs) of 2 km and time space of 3 hours with the interval(Δt) of 5 s are used in the simulation. Origin of the x-y coordinate is taken at the center ($Ic=200$, $Jc=180$) of the grid space and the positive direction of I component in the grid space. Arbitral point(x,y) is connected to a point($r\sin\phi$, $r\cos\phi$) in cylindrical coordinate(r,ϕ). Azimuth angle ϕ is defined as an angle measured from strike in a clockwise direction. At the same time it is connected to grid point(I,J) by(($I-I_c$)Δs,($J-J_c$)Δs).

Accordingly arbitral gird point(I,J) is represented by

$$I = r\sin\phi / \Delta s + I_c$$

$$J = r\cos\phi / \Delta s + J_c$$

Radiation pattern is discussed on the azimuth angle ϕ.

Radiation patterns

Time histories, obtained at points distant from the source($r=340$ km), are shown in Fig.2 for the thrust fault and in Fig.3 for the strike-slip. Time histories of 3 hour were computed but those of 1 hour are shown in the figures. It is understood that the thrust fault generates tsunami. Wavefield of the thrust case is symmetrical to the center line normal to the strike because of the symmetrical pattern of the displacement field. Large amplitude wave with high frequency is detected along the center line. On the other hand small amplitude wave with low frequency is detected along the strike direction. There is a small difference between waveforms at positive and negative directions of x axis. High-frequency predominant wave is seen at the positive direction in comparison with the wave at the negative direction.
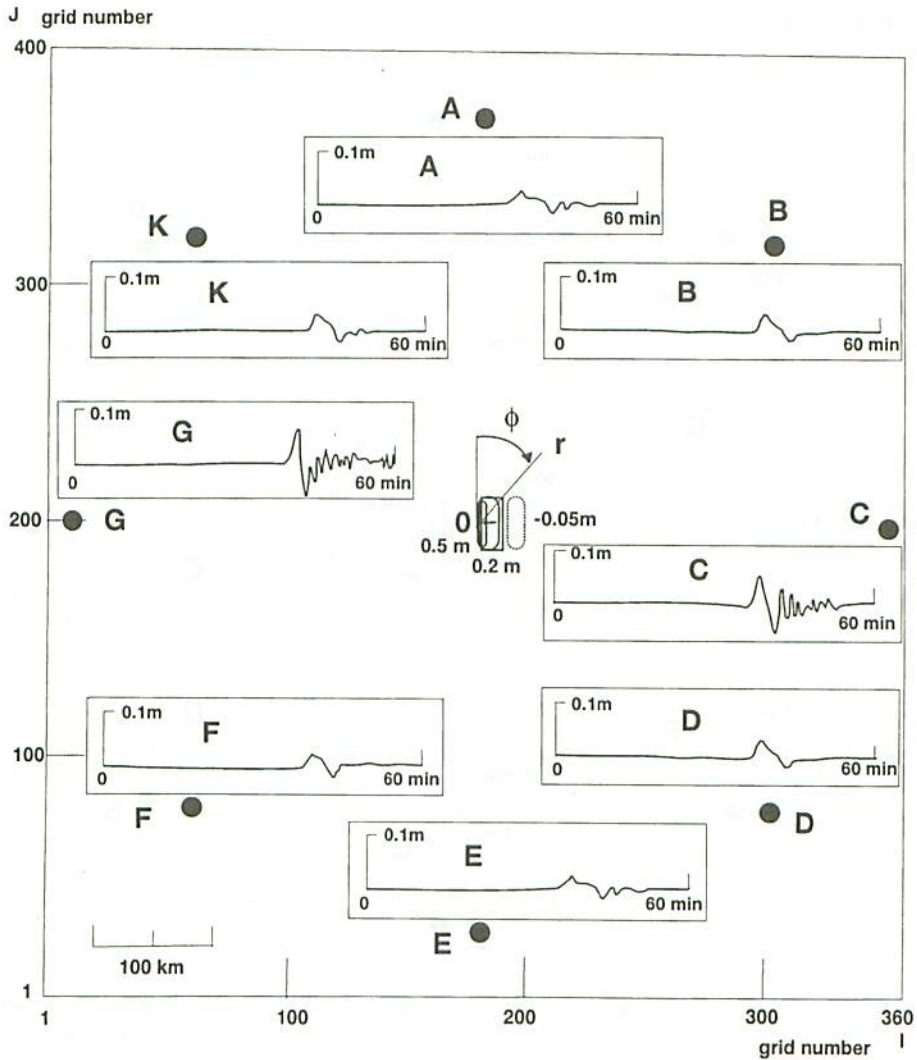
Fig.2 Time histories of sea levels(H) computed for a thrust fault. The vertical displacement at the sea bottom is shown in the figure. Azimuth(ϕ) of a detecting point is defined as an angle from the strike direction.

Wavefield of the strike-slip fault is characterized by no arrival along x axis. It is explained by a superposition of positive wave and negative wave generated at the antisymmetrical displacement field to x axis. It is understood that the same arrival time causes the cancellation. The displacement field slightly differ from quadrant field because of non vertical dip angle($\phi=85°$). Thus, the cancellation is incomplete at the
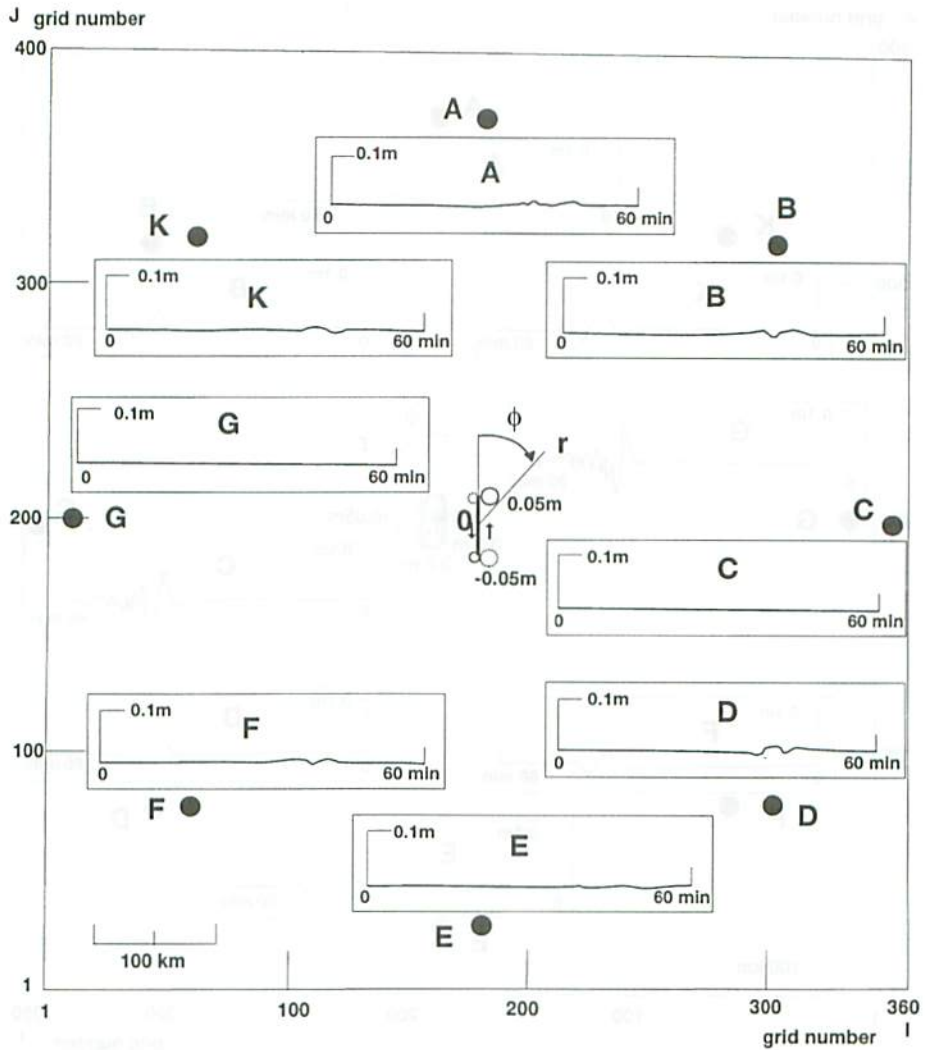
Fig.3   Time histories of sea levels(H) computed for a strike-slip fault. The vertical displacement at the sea bottom is shown in the figure. The azimuth is defined in the same way as in Fig.2.

strike direction.In the strike-slip fault oblique directions are free from the cancellation and tsunami is observed at oblique directions.

Radiation patterns of the maximum levels(H_{max}) in time histories of 3 hours are shown in Fig.4. In both cases they are symmetrical to x axes. But it should be noticed
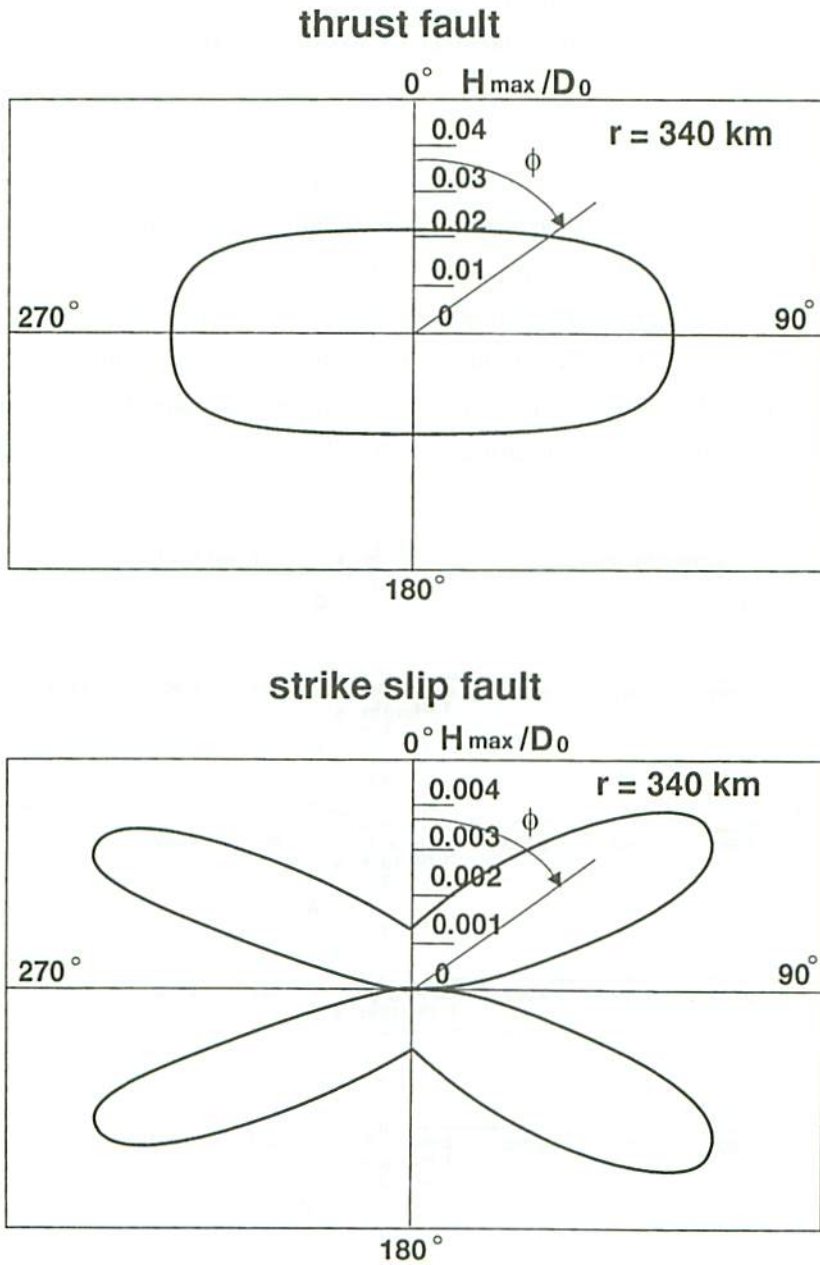
thrust fault

$0°$ H_{max}/D_0

0.04 $r = 340$ km

0.03 ϕ

0.02

0.01

$270°$

$90°$

0

$180°$

strike slip fault

$0° H_{max}/D_0$

0.004 $r = 340$ km

0.003 ϕ

0.002

0.001

$270°$

$90°$

0

$180°$

Fig.4   Azimuth (ϕ) dependencies of the maximum sea levels(H_{max}). Upper figure for the thrust fault and lower one for the strike-slip fault.

that there is a difference of amplitude by about 10 times. In the thrust case they are approximately symmetrical to y axes. The y axes correspond to minimal radiation directions.

Amplitude spectra(a) vs frequency(f) are shown in Fig.5. Goertzel method of spectral estimation was used for the time histories with sampling time of 5 s. The distribution differs place by place. In the spectra of the thrust case the most predominant frequency f_p, frequency at which spectral amplitude take the maximum value, is definitely defined. It is observed that high frequency predominates at normal direction and low frequency at parallel direction. The different excitation is explained from the physical and qualitative differences of length and width. The most predominant frequency is
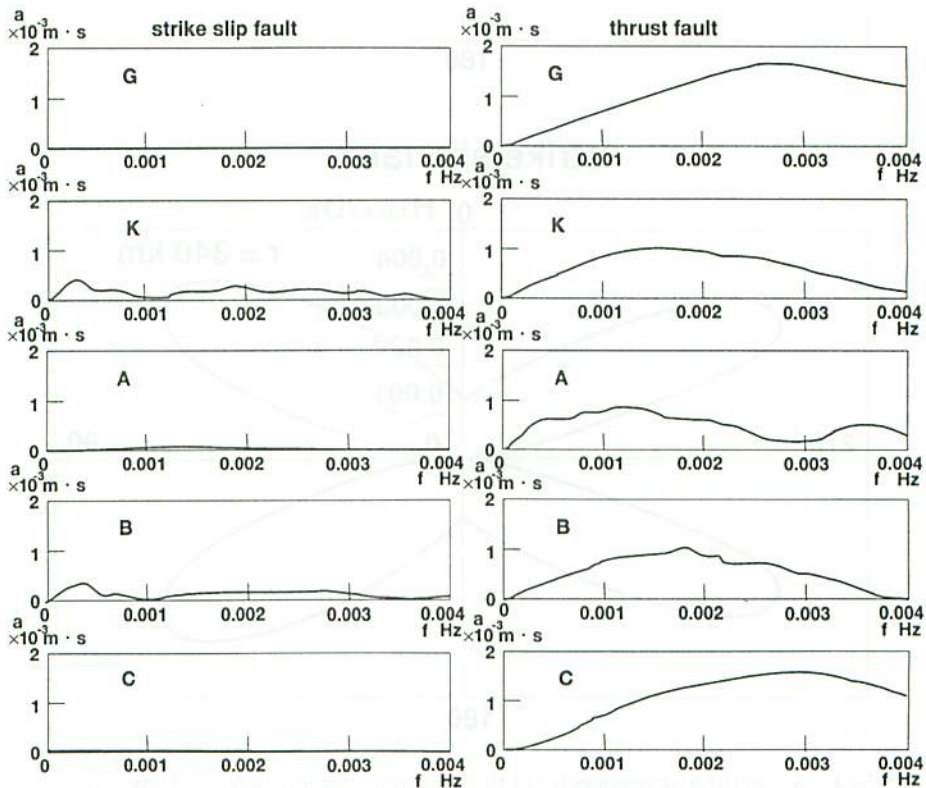

Fig.5　Amplitude spertra(a)for frequency(f).Right one for the thrust fault and left one for the strike-slip fault.

also defined for the strike-slip model.

The most predominant frequencies(f_p) are plotted for the azimuth angles (ϕ) and shown in Fig.6. In the thrust model azimuth dependence of the most predominant frequency
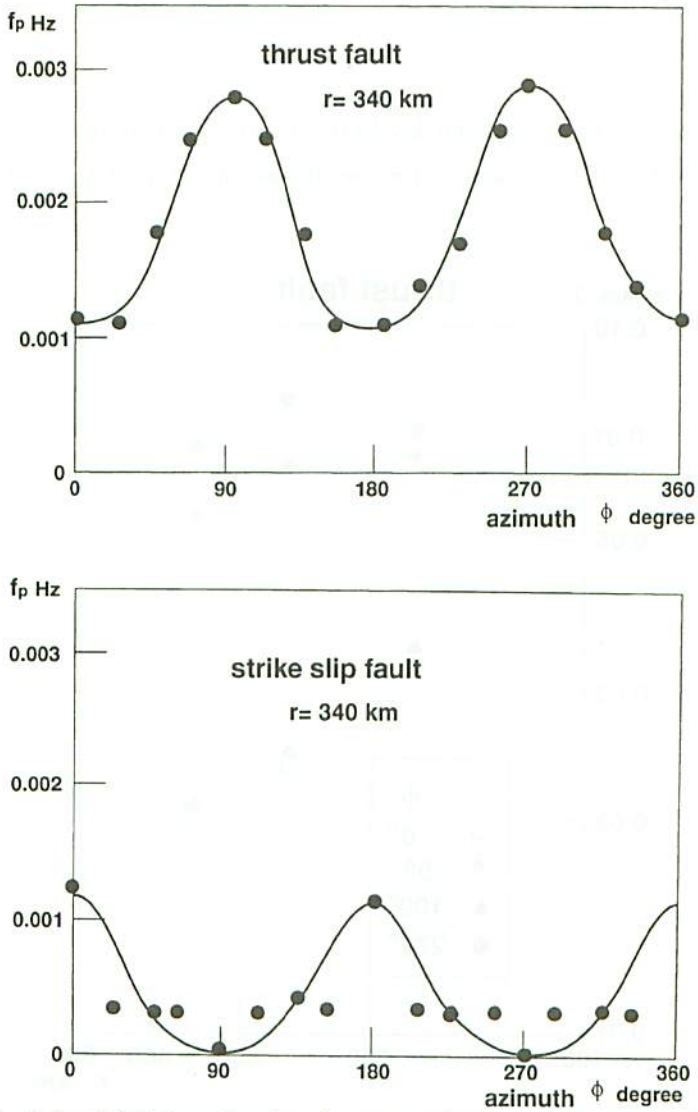

Fig.6 Azimuth(ϕ) dependencies of most predominant frequencies in the spectra. Upper figure for the thrust fault and lower one for the strike-slip fault.

is approximated by $-\cos 2\phi$. On the other hand it is $\cos 2\phi$ in the strike-slip model. The dependencies are clear in the former but ambiguous in the latter.In the strike-slip case the most predominant frequencies are generally low (0.03 Hz). In the thrust case the most predominant frequencies distributes from 0.001 to 0.003 Hz, which are approximately equal to characteristic frequencies of $\sqrt{gh_o}/2\,L$ (0.0014 Hz) and $\sqrt{gh_o}/2\,W$ (0.0028 Hz) defined from source size and tsunami velocity in which g is an acceleration of gravity.

Finally, decrease of the maximum levels(H_{max}) normalized by dislocation(D_o) due to propagation distance(r) are shown for the thrust model in Fig.7. At the normal
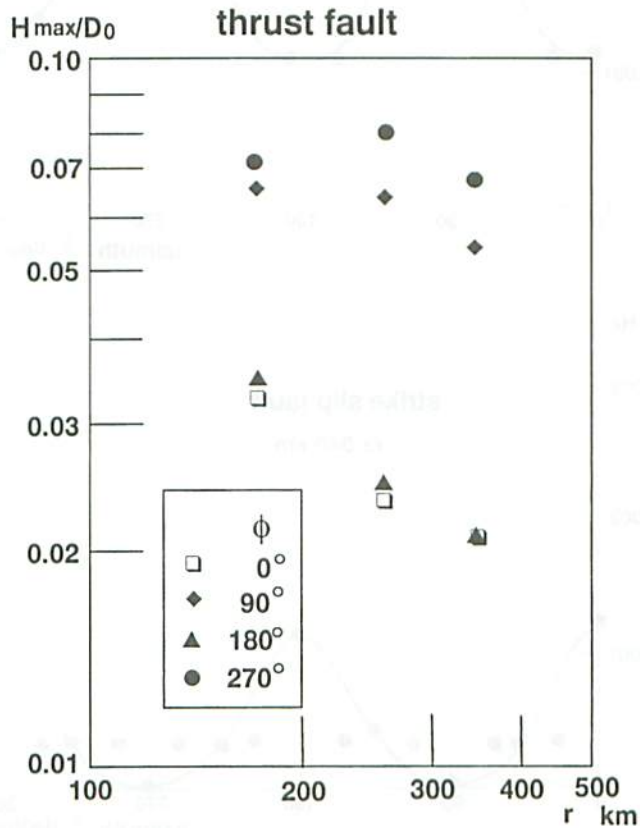

Fig.7 Decreases of the maximum sea levels(H_{max}) to the propagation distances(r) for the thrust fault.

direction the decreasing ratio is 0 or very small. At the parallel direction the decreasing is approximated by $r^{-0.7}$ and the decreasing ratio 0.7 is larger than 0.5 for cylindrical wave.

Discussion

The spectral amplitude can be compared with an analytical expression by Yamashita and Sato(1974). They treat a propagational fault with a finite rupture velocity. In their case we can expect a difference of spectra between opposite directions of fault length, along which the rupture is formed. But the effect is small and it is applicable to our case. Using the corrected formula of their original paper we compared the amplitude spectra. As the result we can obtain the same relative amplitude spectra.

Conclusions

Radiation patterns of tsunami were studied for a thrust fault and a strike-slip fault using numerical simulations. As the result a symmetrical pattern and a quadrant pattern were obtained for the thrust model and strike-slip model, respectively.Moreover, azimuth dependencies of the most predominant frequencies in the spectra were illustrated. Decrease of the maximum sea levels of tsunami was plotted to the propagation distance for the thrust model. In the normal direction the decrease was very small and the maximum radiation is explained from the small decrease. The radiation patterns suggest that the superposing condition, that is the phase difference between two waves coming from both sides of the observation point, has an important role.

References

Aida, I., 1978, Reliability of a tsunami source model derived from fault parameters,J.Phys. Earth,26,57-73.

Abe, Ku.,1993, Tsunami spectra as a synthesis of source spectrum and shelf
    response, Proceed. IUGG/IOC International Tsunami Sympo.,151-163.

Abe, Ku.,1996, Source model of the 1946 Aleutian Tsunami derived from the predominat
    frequencies, Science of Tsunami Hazards,14,71-78.

Abe, Ku. and M. Okada, 1995 a, Source model of Noto-Hanto-Oki earthquake
    tsunami of 7 February 1993,PAGEOPH,144,621-631.

Abe, Ku. and M. Okada, 1995 b,Source model of Hokkaido-toho-oki earthquake tsunami,
    Abst. Japan Earth and Planet. Sci. Joint Meet., 140,(in Japanese).

Abe, and M. Okada, 1997, Tsunami generation of the 1995 Hyogoken–nanbu(Kobe)
    earthquake, J. Natural Disaster Science, 18, in press..

Hatori, T., 1963, Directivity of tsunami, Bull.Earthq. Res. Inst.,Tokyo Univ., 41,61-81.

Mansinha, L. and D. E. Smylie, 1971,Displacement fields of inclined faults,
    Bull. Seismol. Soc. Am., 61,1433-1440.

Matsuzawa, T., 1937, Directivity of tsunami, Zisin, 1,9,23-25(in Japanese).

Miyoshi, H., 1955, Directivity of the recent tsunami, Journ. Oceanogr. Soc. Japan,11,
    151-155.

Momoi, T., 1962, The directivity of tsunami(1)–The case of instantaneous and uniformly
    elevated elliptic wave origin, Bull. Earthq. Res. Inst., Tokyo Univ., 40,297-307.

Yamashita, T. and R. Sato, 1974, Generation of tsunami by a fault model,J.
    Phys. Earth, 22,415-440.